Journal of Chromatography A, 1217 (2010) 2013–2021

Contents lists available at ScienceDirect

Journal of Chromatography A

journal homepage: www.elsevier.com/locate/chroma

Experimental implementation of automatic 'cycle to cycle' control to a nonlinear chiral simulated moving bed separation

Cristian Grossmann[a], Christian Langel[b], Marco Mazzotti[b,*], Manfred Morari[a], Massimo Morbidelli[c]

[a] ETH Zurich, Automatic Control Laboratory, Physikstrasse 3, 8092 Zurich, Switzerland
[b] ETH Zurich, Institute of Process Engineering, Sonneggstrasse 3, 8092 Zurich, Switzerland
[c] ETH Zurich, Institute for Chemical and Bioengineering, Wolfgang-Pauli-Str. 10, 8093 Zurich, Switzerland

ARTICLE INFO

Article history:
Received 11 May 2009
Received in revised form 6 January 2010
Accepted 22 January 2010
Available online 1 February 2010

Keywords:
Simulated moving bed
Nonlinear chiral separation
On-line monitoring
Cycle to cycle
Optimizing control

ABSTRACT

In order to better exploit the economic potential of the simulated moving bed chromatography a 'cycle to cycle' controller which only requires the information about the linear adsorption behavior and the overall average porosity of the columns has been proposed. Recently, an automated on-line HPLC monitoring system which determines the concentrations in the two product streams averaged over one cycle, and returns them as feedback information to the controller was implemented. The new system allows for an accurate determination of the average concentration of the product streams even if the plant is operated at high concentrations. This paper presents the experimental implementation of the 'cycle to cycle' control concept to the separation of guaifenesin enantiomers under nonlinear chromatographic conditions, i.e. at high feed concentrations. Different case studies have been carried out to challenge the controller under realistic operation conditions, e.g. introducing pump disturbances and changing the feed concentration during the operation. The experimental results clearly demonstrate that the controller can indeed deliver the specified purities and improve the process performance.

1. Introduction

Simulated moving bed (SMB) chromatography is a continuous separation process that is generally used to separate a feed mixture into two fractions. In SMB chromatography the movement of the solid phase is simulated by periodically switching the inlet and outlet ports of the unit in the direction of the fluid flow, as illustrated in Fig. 1. Compared to batch chromatography SMB allows to achieve higher productivity and to reduce the solvent consumption due to its countercurrent operation principle.

For the separation of fine chemicals and the production of single enantiomer drugs SMB has become a widely applied technique [1]. The strict regulations on the purity constraints of chiral drugs imposed by the US Food and Drug Administration (FDA) and the European Medicines Agency (EMEA) have increased the demand for single enantiomer drugs over the last years. However, it still remains a challenge for SMB practitioners to fulfill the purity requirements and at the same time to optimize the productivity of the process. As a consequence SMB units are often operated without exploiting the full economic potential of the process to guarantee the process specifications.

In the literature different control schemes have been proposed over the last years to optimize the operating conditions to utilize the full economic potential of the SMB process [3–12]. However, the drawback of most of these approaches is the need for accurate adsorption measurements prior to the development of the controller.

A significant feature of the controller developed at ETH Zurich is that it requires only minimal information about the system, namely the overall void fraction of the columns and the linear adsorption behavior of the mixture to be separated. It has been proven by extensive simulations that the controller is able to fulfill the process specifications and to optimize the separation performance for mixtures subject to linear, Langmuir [14] and generalized Langmuir [15] isotherms. The effectiveness of the controller has also been demonstrated experimentally, on achiral systems subject to linear isotherms [16] and on chiral systems with Langmuir isotherms [17], but never reaching high feed concentrations as it is the case in this work.

A critical issue encountered in the separation of chiral compounds is how to monitor the concentration of both enantiomers in the two product streams, extract and raffinate. These concentration measurements are essential since they are required as feedback information by the controller. Noisy and bad quality measurements will give poor control performance no matter how sophisticated the control technique might be. Recently, an automated on-line HPLC monitoring system for the 'cycle to cycle' controller was developed

* Corresponding author. Tel.: +41 44 6322456; fax: +41 44 6321141.
E-mail address: marco.mazzotti@ipe.mavt.ethz.ch (M. Mazzotti).

0021-9673/$ – see front matter © 2010 Elsevier B.V. All rights reserved.
doi:10.1016/j.chroma.2010.01.074

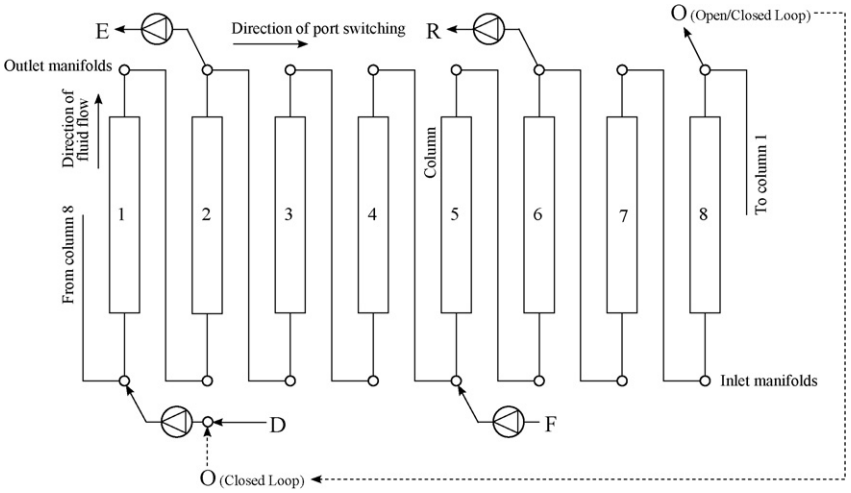

Fig. 1. Scheme of the 2-2-2-2 laboratory scale SMB plant.

and implemented [18]. The new on-line monitoring technique is based on HPLC measurements of the average concentrations of the two product streams during one cycle, i.e. a time corresponding to a number of port switches equal to the number of columns, and thus it overcomes the limitations imposed by optical detectors on the performance of the controller for chiral SMB separations [17]. The system allows us to monitor the concentrations in the product streams even if the plant is operated at high feed concentrations.

This work presents the experimental implementation and results of the 'cycle to cycle' optimizing controller for a high purity chiral SMB separation under nonlinear chromatographic conditions, i.e. at high feed concentrations. This is an important achievement since it is well known that the productivity of an SMB unit increases with the total feed concentration and therefore, this regime is the most interesting in practice, particularly for pharmaceutical applications and chiral separations. The paper is organized as follows: in the second section, a brief overview of the operation of SMB units at high feed concentrations and of the SMB optimizing control concept is presented. In the third section, the experimental setup is described. Finally, the performance of the controller is assessed and discussed for the separation of the enantiomers of the chiral compound guaifenesin at high feed concentrations.

2. Background

2.1. Optimal SMB operation at high total feed concentrations

This section aims at illustrating the effect of the feed concentration on the SMB operation. The impact of the total feed concentration on the optimal operation of an SMB process is exemplarily analyzed for the separation of a mixture characterized by a generalized Langmuir isotherm [19]. To present and illustrate the ideas and further on the experimental results the "triangle theory" is used, a well established method to design SMB separations and to interpret SMB results [19,20].

In the frame of the triangle theory it can be demonstrated that at steady state conditions the key design parameters influencing the separation performance of an SMB are the dimensionless flow rate ratios m_j, which are defined as follows [21]:

$$m_j = \frac{Q_j t^* - V\epsilon^*}{V(1-\epsilon^*)} \qquad (j = 1, \ldots, 4). \tag{1}$$

In the above equation V, t^*, Q_j and ϵ^* are the column volume, the switch time, the flow rate in section j and the overall bed void fraction, respectively. The following criteria for the choice of the flow rate ratios m_j, which if fulfilled lead to complete separation, can be derived [19,21]:

$$m_{1,\min} < m_1 \tag{2}$$

$$m_{2,\min} < m_2 < m_{2,\max} \tag{3}$$

$$m_{3,\min} < m_3 < m_{3,\max} \tag{4}$$

$$m_4 < m_{4,\max} \tag{5}$$

It should be noted that in general all the upper and lower bounds are functions of m_2 and m_3, the adsorption isotherm parameters and the feed concentration. A detailed analysis, derivation and description of the boundaries can be found in the literature [19,22].

The separation conditions can be graphically represented in a plane spanned by the flow rate ratios m_2 and m_3. Fig. 2 shows the (m_2, m_3) plane for an arbitrary Langmuir-type isotherm, where complete separation regions are plotted for increasing feed concentrations as indicated by the arrow. The case of infinite dilution is represented by the solid triangle, whose upper and lower bounds are given by the Henry constants of the more and less retained component H_A and H_B, respectively. As the feed concentration is increased the triangle becomes more and more narrow and bends downwards to the left (dashed lines in Fig. 2).

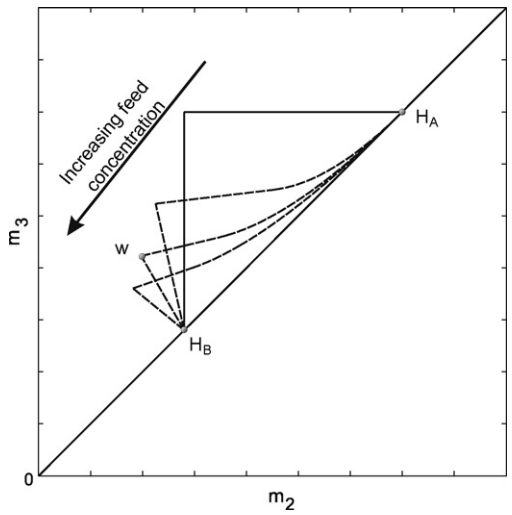

Fig. 2. Effect of increasing total feed concentration on the separation conditions on the (m_2, m_3) plane. The point **W** achieves the maximal feed flow rate under complete separation conditions.

Operating an SMB unit optimally is regarded in this work as maximizing the feed throughput and minimizing the solvent consumption while fulfilling the specified purities. The productivity is defined as the amount of component separated per unit time and per unit volume of stationary phase and can be written by applying Eq. (1) as follows:

$$PR = \frac{Q_F c_T^F}{n_{\text{col}} V (1-\epsilon^*)} = \frac{(m_3 - m_2) c_T^F}{n_{\text{col}} t^*}, \tag{6}$$

where Q_F, c_T^F and n_{col} are the feed flow rate, the overall feed concentration and the number of columns in the SMB unit, respectively.

The solvent consumption is defined as the amount of solvent required per amount of mixture separated:

$$SC = \frac{Q_D + Q_F}{Q_F c_T^F} = \frac{m_1 - m_4 + m_3 - m_2}{(m_3 - m_2) c_T^F}, \tag{7}$$

where Q_D is the solvent flow rate. It can easily be seen that for a constant switch time t^* and a given mixture with constant overall feed concentration c_T^F, the productivity PR and the solvent consumption SC improve by increasing the term $(m_3 - m_2)$. Therefore, the point in the (m_2, m_3) plane that maximizes productivity and achieves complete separation for a given c_T^F is the vertex of the triangle, where m_2 and m_3 are as small and as large as possible, respectively. This point is denoted as **W** for one of the triangles in Fig. 2 and moves down to the left in the (m_2, m_3) plane as the total feed concentration is increased.

2.2. Cycle to cycle optimizing control

This section presents the main ideas of the 'cycle to cycle' control concept. A detailed description of the theory behind the controller has been extensively reported [23]. The control concept is based on Model Predictive Control (MPC) [26]. An important element of the controller is an explicit and simplified SMB model that requires only the linear isotherm coefficients and the averaged overall bed porosity of the columns. These parameters can be easily obtained from pulse injection experiments under diluted conditions.

The simplified SMB model is obtained by applying a number of simplification steps to an SMB model. The SMB model is based on first principles and comprises partial differential equations describing the dynamics of each chromatographic column, algebraic equations describing the connections among them as well as the proper boundary and initial conditions. The equilibrium dispersive model is used to describe the dynamics inside each chromatographic column:

$$\frac{\partial c_{i,h}}{\partial t} + \frac{(1-\varepsilon_h)}{\varepsilon_h}\frac{\partial q_{i,h}^*}{\partial t} + \frac{Q_h}{A_{cr}\varepsilon_h}\frac{\partial c_{i,h}}{\partial z} = D_{ap,i}\frac{\partial^2 c_{i,h}}{\partial z^2} \quad \text{for } i = A, B \quad h = 1, \ldots, n_{\text{col}} \tag{8}$$

In the above equation, $D_{ap,i}$ is the apparent axial dispersion coefficient lumping the mass-transfer resistance and axial dispersion; ε_h is the total packing porosity in the h th column; $c_{i,h}$ is the fluid phase concentration and $q_{i,h}^*$ is the equilibrium solid phase concentration of component i in column h; A_{cr} is the column cross-section area. The variable Q_h is the flow rate in column h of the SMB unit.

The adsorption behavior of both components inside the columns is assumed to follow a linear adsorption isotherm $q_{i,h}^* = H_i c_{i,h}$, with Henry's constants H_A and H_B, where A and B are the strongly and weakly adsorbed components, respectively. Note that Eq. (8) is still nonlinear due to the convective term where the flow rate (input variable) is multiplied by the derivative of the concentration (state variable). Such nonlinear SMB model is simplified through a number of steps to a linear discrete-time reduced order dynamical model which will be referred to as simplified SMB model. The details of the simplification steps have been reported elsewhere [23]. The simplified SMB model has the general form:

$$\begin{aligned} x_{k+1} &= Ax_k + Bu_k \quad x \in \mathbf{R}^{n_x},\ u \in \mathbf{R}^{n_u} \\ y_k &= Cx_k + Du_k \quad y \in \mathbf{R}^{n_y} \end{aligned} \tag{9}$$

where A, B, C and D are the system matrices that form the state-space model and contain the information about the dynamics of the system at the linearization point [23]. The vectors x, u and y are the state, input and output of the model of dimensions n_x, n_u and n_y, respectively. The index k is the cycle index.

A disturbance model is included in the simplified SMB model in order to account for the unavoidable mismatch between the linear dynamics and the full nonlinear SMB model describing the real experimental plant, i.e. the plant model mismatch. Besides, the disturbance model captures the combined overall effect of all possible disturbances on the plant output which is a critical issue for the control performance. The disturbances affecting SMB units can be divided into two categories. The first one are persisting periodic disturbances with period of one cycle, e.g., changes in the feed concentration during operation due to different feed batches of the mixture to be separated. This kind of disturbances will persist throughout the operation. The second category consists of random disturbances which do not repeat every cycle. The effect of unknown model errors and both type of disturbances are incorporated as a residual term in the state vector x which will be estimated using a Kalman filter. The measured variables or outputs y are the product (extract and raffinate) concentrations averaged over one cycle. The manipulated variables or inputs u are the four internal flow rates in the four sections of the SMB unit. The switching time, t^*, is fixed in this work, it is predefined and chosen based on maximum allowable pressure drop considerations. It is worth noting, however, that the switching time has an effect on the productivity, which could be exploited by the controller for SMB optimization as shown elsewhere [8,27]. More details on the cycle to cycle controller can be found elsewhere [23].

With the simplified SMB model the controller is able to predict the future evolution of the SMB plant. Based on this the controller calculates a set of manipulated variables, i.e. flow rates, which is optimal with respect to the specified objective function, and fulfills the given product and process constraints according to the simplified SMB model. A significant feature of the controller is that its simplified SMB model requires *only* the linear isotherm information, i.e. H_A and H_B, and the overall bed porosity ϵ^* of the columns.

Due to the model-based nature of the controller it is straightforward to impose the operational constraints and the process specifications in straightforward manner within the control formulation. The controller has to fulfill two main tasks: the first and most important task of the controller is to achieve the desired minimal purities in the product streams; the second task will be to optimize the unit with respect to the cost function, or performance index. The constraint on the minimal purity specifications can be formulated as:

$$\begin{aligned} P_E^{\text{ave}} &\geq P_E^{\min} - s_1 \\ P_R^{\text{ave}} &\geq P_R^{\min} - s_2, \end{aligned} \tag{10}$$

where P_E^{ave} and P_R^{ave} are the extract and raffinate purities, respectively, averaged over one cycle. The non-negative slack variables s_1 and s_2 are introduced to soften the constraints on the purity specifications and to avoid infeasibility problems [23]. In order to check whether the conditions in Eq. (10) are fulfilled or not, the controller receives once per cycle the results of the concentration measurements of the two product streams. Based on this information the controller will compute the actions to be undertaken for the next process cycle.

The process constraints such as the maximal pressure drop in the unit are considered by constraining the manipulated variables

with upper bounds. The maximal rate of change of the manipulated variables is constrained as well to avoid sudden and large pressure fluctuations in the unit:

$$\begin{aligned} &Q_j \le Q^{\max} \\ &|\Delta Q_j| \le \Delta Q^{\max} \qquad (j = 1, \ldots, 4), \end{aligned} \tag{11}$$

where $|\Delta Q_j|$ is the flow rate change in section j from one cycle to the next cycle.

The second task to be pursued is the optimization of the performance of the SMB plant by maximizing the productivity and by minimizing the solvent consumption as defined by Eqs. (6) and (7), respectively. Therefore, the cost function of the optimization problem is required to minimize a weighted sum of productivity and solvent consumption over one cycle and the slack variables:

$$\min_{Q_1,\ldots,Q_4,\mathbf{s}} [(\lambda_D Q_D - \lambda_F Q_F) + \lambda_s \mathbf{s}] \tag{12}$$

The weights λ_F and λ_D reflect the relative importance given to maximizing the productivity or to minimizing the desorbent consumption, respectively; the vector λ_s contains the weight for the slack variables and the vector $\mathbf{s}$ contains the slack variables itself. Note that beside those in Eq. (10), other slack variables are introduced to avoid negative values of the predicted concentrations and to minimize changes in the operating conditions for the sake of a smooth operation. A discussion on how the weights in the cost function steer the controller's behavior has been reported previously [15].

The linear cost function of Eq. (12) together with the simplified SMB model in Eq. (9) and the linear constraints Eqs. (10) and (11) constitute a linear programming (LP) problem solved online once every cycle, i.e. from 'cycle to cycle'. ILOG CPLEX 10.0 (ILOG, Sunnyvalle CA, USA) is a commercial LP solver and was used online with a computation time of about 0.1 s on a PC with a 3 GHz processor. A detailed description of the solution method, including a discussion of some implementation issues that are not reported here for the sake of brevity, may be found elsewhere [23].

3. Experimental

3.1. Materials

A racemic mixture of guaifenesin (Fludan, Vankleek Hill, Canada) enantiomers was separated using CHIRALCEL™ OD (Chiral Technologies Europe, Illkirch, France) as stationary phase and pure ethanol as mobile phase. This cellulose based chiral stationary phase (cellulose tris (3,5-dimethylphenylcarbamate) coated on silica) is designed for high performance separations and has a particle size of 20 μm. The material was slurry packed into stainless steel columns using a mobile phase mixture of 95/5% (v/v) ethanol and 2-propanol with a flow rate of $Q = 46$ ml/min and 40 min packing time. The pressure drop across the column during packing was 36 bar, which is within the maximum allowable pressure of 40 bar for this stationary phase.

3.2. Laboratory SMB unit

The laboratory SMB unit comprises 8 semi-preparative columns (10 cm length, 1 cm diameter) with 2 columns in every section (2-2-2-2 configuration) and is located in a room with climate control for isothermal operation at $T = 23\,^{\circ}$C. The unit is operated in a closed loop mode (see Fig. 1). In order to account for the effect of the extra-column dead volume, the flow rate ratios m_j are calculated as follows [24]:

$$m_j = \frac{Q_j t^* - V\epsilon^* - V_j^D}{V(1-\epsilon^*)} \qquad (j = 1, \ldots, 4), \tag{13}$$

Table 1
Results of the column pulse injections with ethanol mobile phase at 23 °C; $c_A = c_B = 0.01$ g/L; V_{inj} μl.

Column no.	H_B	H_A	ϵ^*
1	0.51	1.10	0.75
2	0.49	1.10	0.75
3	0.50	1.10	0.74
4	0.48	1.06	0.75
5	0.52	1.12	0.75
6	0.51	1.10	0.75
7	0.48	1.08	0.74
8	0.51	1.10	0.74
Average	0.50	1.10	0.75

where V_j^D is the extra-column dead volume in section j. For all four sections of our SMB unit $V_j^D = 0.133$ ml. A detailed analysis and description of how to account for the dead volume can be found in an earlier publication [25].

3.3. Characterization

In accordance with the purpose of this paper, namely to demonstrate that with the proposed controller the knowledge of the complete adsorption isotherm is not required to operate an SMB unit fulfilling the process and product constraints, only the linear adsorption behavior of the guaifenesin enantiomers was determined at $T = 23\,^{\circ}$C. First, the overall void fraction ϵ^* was determined by measuring the retention time of a non-retained compound, in this case a solvent mixture in pure ethanol. Note that t_0 is obtained subtracting the dead time of the HPLC system from the retention time of the non-retained compound:

$$\epsilon^* = \frac{t_0 Q}{V}, \tag{14}$$

where Q and V are the volumetric flow rate and the column volume, respectively. The Henry constants H_i of the two enantiomers were calculated from the retention time of the two components obtained under diluted conditions:

$$H_i = \frac{\epsilon^*}{1-\epsilon^*}\left(\frac{t_{R,i} - t_0}{t_0}\right) \qquad (i = A, B). \tag{15}$$

Here, $t_{R,i}$ is the residence time of component i corrected with the dead time of the HPLC system. Table 1 reports the results for the 8 columns together with the averaged values. The latter will be used for the calculations and the graphical representations in the (m_2, m_3) plane.

3.4. On-line monitoring

In past works a combination of optical detectors, i.e. UV absorbance detector and polarimeter was used to determine continuously the average concentrations in the product streams. Relying on these measurement techniques involved a substantial effort to circumvent inherent limitations of the optical detectors as discussed elsewhere [17].

In the present work a recently developed automated on-line HPLC monitoring system (referred as AMS) was used. A detailed description and validation of this system were reported earlier [18]. For the sake of completeness, the main ideas and working principles of the on-line monitoring system are summarized here.

The AMS is custom-made and consists of two main parts, namely a conventional HPLC unit (Agilent LC 1200, Santa Clara, USA) combined with an automated sample collecting system developed for the SMB process (see Fig. 3), that consists of four glass tanks; two tanks (E1 and E2) designated to alternately collect the extract stream, and two others for the raffinate stream (R1 and R2).

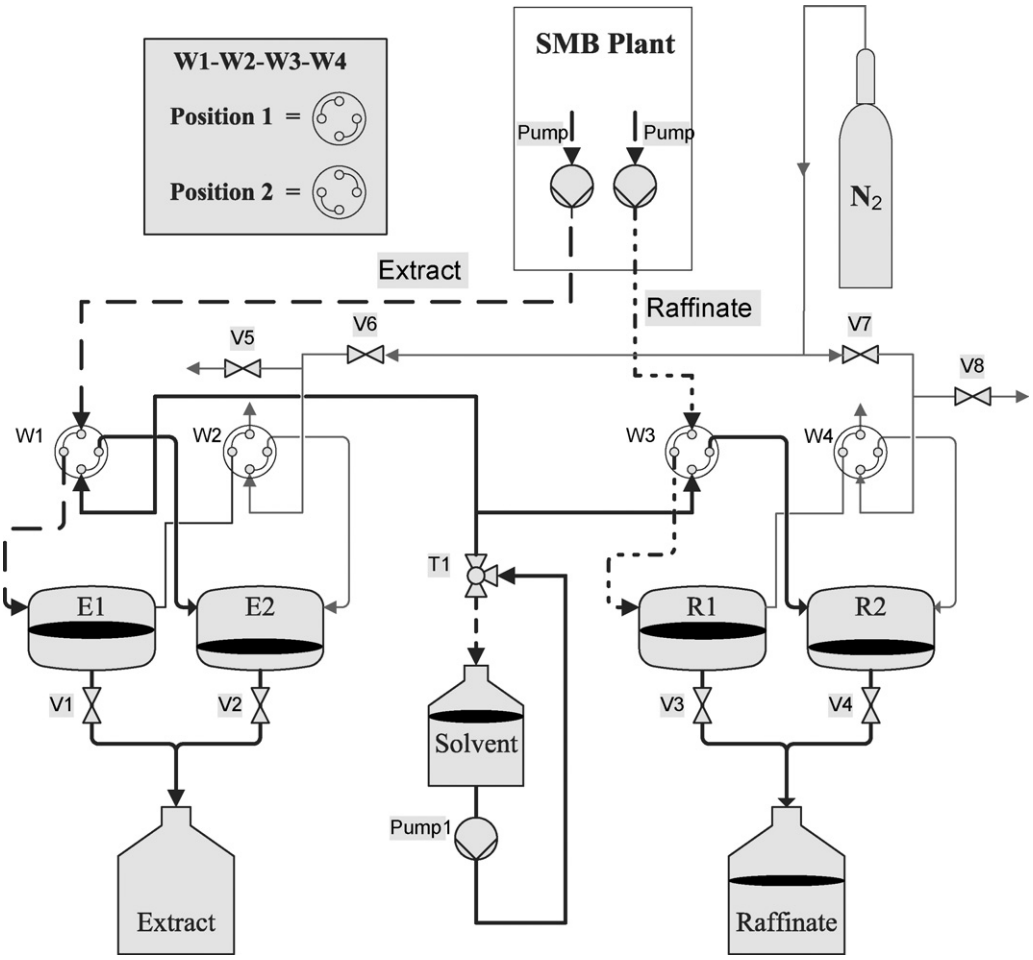

Fig. 3. Process flow sheet for the automated on-line HPLC monitoring system. Position 1 and Position 2 indicate the possible valve positions for W1–W4. Thick lines indicate fluid flow and thin lines gas flow.

During the odd cycles of the process the product streams are collected in tanks E1 (extract) and R1 (raffinate), whereas for analysis from tanks E2 and R2 (filled up in the previous cycle) a sample is injected into the HPLC. The two samples are injected with a time difference long enough to avoid overlapping of the peaks; extract is always injected first. Once the injections have been performed, tanks E2 and R2 are flushed and cleaned to be ready for the next collecting period. The HPLC automatically analyzes the chromatograms and returns the concentration values for the two components in both product streams, i.e. the feedback information for the controller. In the even cycles the situation is vice versa with respect to the tanks; from E1 and R1 samples are injected to the HPLC system, while E2 and R2 are used to collect the product streams.

The time required for HPLC analysis of the samples needs to be smaller than the cycle time of the SMB process, otherwise the HPLC would not be ready for the next sample injection at the beginning of a new cycle. Therefore, the injection procedure needs to be tuned to fulfill this constraint. A good compromise between retention time and peak resolution was found at a solvent composition of 60/40% (v/v) ethanol and heptane with a flow rate of $Q = 0.73$ ml/min using an analytical Chiralcel OD column (25 cm length, 0.46 cm diameter). The analytical column is located in a temperature controlled column compartment and kept at 23 °C. Note that this monitoring system allows us to use different mobile phases and stationary phases for the analysis in the HPLC and for the separation in the SMB unit. However, it has to be pointed out that using a different mobile phase composition in the SMB and the HPLC can create additional solvent peaks in the chromatogram. When designing the analyzing procedure, it has to be guaranteed that possible solvent peaks do not interfere with the peaks of the two components to be separated, in order to avoid a loss of accuracy in the feedback to the controller.

4. Results and discussion

The main result of this paper, case study 1, investigates the effect of the feed concentration on the final operating point. Therefore, a series of six experiments with increasing total feed concentration ranging from 0.75 to 18 g/L was carried out. The second and third case study aim at demonstrating the independence of the final operating point of the initial conditions as well as to assess the controller performance for disturbance rejection at high feed concentrations. The last case study presents a separation with very high purity requirements, i.e. above 99%.

The simplified SMB model of the controller is based on the information about the linear adsorption isotherm of the system to be separated, i.e. only the Henry constants and the average overall void fraction of the columns. However, at high total feed concentrations the adsorption behavior becomes nonlinear. Besides, temperature deviations, extra-column dead volume, and aging of the stationary phase affect the retention behavior of the compounds to be separated. In order to mimic these realistic process uncertainties a plant/model mismatch was introduced, i.e. the controller was developed using different Henry constants than those measured earlier, i.e. $H_A = 1.10$ and $H_B = 0.50$. Thus, in all the cases presented

Table 2
Total feed concentrations of runs A–F together with the initial and final operating conditions for runs A–F in terms of m_j ($j = 1, \ldots, 4$) and the final value of the productivity *PR*. The initial values of run C′ correspond to the final values of run D. Run C″ reports the values of the SMB unit right after the disturbance and once it has been rejected in case study 3.

Run	c_T^F	Initial values				Final values				*PR*
	[g/L]	m_1	m_2	m_3	m_4	m_1	m_2	m_3	m_4	[g/(min L)]
A	0.75	1.199	0.233	1.048	0.272	1.272	0.458	0.954	0.174	0.023
B	4.0	1.212	0.334	1.097	0.303	1.229	0.447	0.916	0.192	0.117
C	8.0	1.212	0.334	1.04	0.303	1.235	0.422	0.884	0.189	0.231
C′	8.0	1.243	0.414	0.876	0.182	1.243	0.421	0.883	0.182	0.231
C″	8.0	1.408	0.596	1.059	0.361	1.413	0.437	0.889	0.165	0.226
D	10.0	1.211	0.334	0.996	0.303	1.243	0.414	0.876	0.182	0.289
E	14.0	1.211	0.334	0.975	0.232	1.180	0.401	0.844	0.105	0.388
F	18.0	1.211	0.334	0.955	0.303	1.312	0.396	0.833	0.123	0.492

below the controller was designed using $H_A = 1.25$ and $H_B = 0.61$. The difference corresponds to an error of 13% and 22%, respectively, and is well above the typical measurement error. Note that the complete adsorption behavior of the system to be separated has neither been measured, nor it is known from the literature.

4.1. Case study 1: controlled SMB operation at high total feed concentrations

The aim of this section is to demonstrate that the controller can deliver the specified purities and improve the process performance with the knowledge of the linear adsorption behavior only, even if the separation under investigation is governed by an unknown nonlinear adsorption isotherm.

Six different experiments were carried out with total feed concentrations of 0.75, 4.0, 8.0, 10.0, 14.0, and 18.0 g/L. For all the runs the same minimal purity requirements were specified for both product streams, namely 98.5%. This allows to track the final operating point of each control run and makes the comparison among them easier. The unit was always started up with initially clean columns, i.e. before each experiment the unit was carefully flushed with pure solvent to completely remove any adsorbed compound. All experiments were carried out at a constant switch time of $t^* = 2.00$ min, and the initial and final operating conditions in terms of m_j ($j = 1, \ldots, 4$) are listed in Table 2. The same configuration of the controller was used in all six experiments with the controller switched on at cycle 5.

Fig. 4a–f shows the time evolution of extract and raffinate purities, and of the performance index (*P.I.*) as a function of the cycle number together with the trajectories of the operating conditions in the (m_2, m_3) plane for the six runs A–F. The performance index to be minimized by the controller, as defined in Eq. (12), is the same for all the cases, with $\lambda_F = 20$, $\lambda_D = 4$ and $\lambda_s = (1000, 1000)$. The performance index plotted in all the figures contains only the economic terms and not the slack variables.

From Fig. 4 a–f, it is apparent that for all experiments the minimum purity specification is fulfilled within less than 40 cycles and even faster in the cases of runs A, B, C and D. The final operating points reached by the controller and that fulfill the purity specifications of 98.5%, are shown in the (m_2, m_3) plane of Fig. 4 a–f and are denoted with a different marker for each of the runs. Plotting all the final operating points of runs A–F together in the (m_2, m_3) plane as in Fig. 5 allows to identify a trend among them: with increasing feed concentration the final operating point that fulfills a given purity shifts towards the lower left corner of the (m_2, m_3) plane, i.e. towards the origin. This is the same trend predicted by the "triangle theory" for the point of maximal productivity and complete separation "**W**", for systems with Langmuir-type adsorption behavior, as discussed in Section 2.1 and illustrated in Fig. 2. The productivity values reported in Table 2 were calculated using Eq. (6), together with the final values of m_2 and m_3. From Table 2, it is apparent that the productivity *PR* at steady state conditions increases with the total feed concentration from run A–F. This result is expected for a system following a Langmuir-type adsorption behavior [21].

Two important conclusions can be drawn from this set of experiments. First, these results clearly demonstrate the capability of the controller to fulfill the process and product specifications whatever the feed concentration is and regardless of the adsorption behavior that governs the SMB process. Secondly, the impact of increasing the feed concentration on the final operating point has been demonstrated experimentally and is at least qualitatively consistent with that predicted by the "triangle theory" for systems governed by a Langmuir-type adsorption isotherm. The results presented here represent a major improvement compared to previously presented experimental results where the operation at high feed concentrations was made very difficult due to limitations of the monitoring device [17].

4.2. Case study 2: change of feed concentration during operation

Let us now check, whether the final operating point reached by the controller in the (m_2, m_3) plane is unique for the same feed concentration when two different initial points are considered. To address this question one of the runs presented in the previous case study, namely run D, was subjected to a disturbance after reaching its final operating point.

More specifically, the total feed concentration was modified to that of run C, i.e. it was decreased at cycle 105 from 10 g/L (run D) to 8 g/L (run C). Fig. 6a shows the time evolution of the extract and raffinate purities and the performance index *P.I.* as a function of the cycle number. Fig. 6b reports the corresponding operating trajectory for experimental run D. As a result of the change in feed concentration, the extract purity drops below the specifications but is recovered within less than 20 cycles, whereas the raffinate purity increases (see Fig. 6a). The difference between the raffinate purity and the minimum specified purity reflects the gap that can be exploited by the controller for optimization.

In the first part of experimental run D, the controller drives the operation from the initial point to the final operating point indicated with D, as can be seen in Fig. 6b. Once the feed concentration has been changed to 8 g/L, the controller successfully rejects the disturbance and moves the operating point to the position denoted with C′. For comparison the end point of experimental run C, i.e. for the experiment where the SMB unit was started up with clean columns and a feed concentration of $c_T^F = 8$ g/L from the beginning, is plotted as well and denoted as C. The two final operating points C and C′ overlap, as demonstrated also by the final m_2 and m_3 values listed in Table 2. This result demonstrates that the final operating point in the (m_2, m_3) plane fulfilling the specified purity is unique and can be reached by the controller within the experimental accuracy independently of the initial conditions.

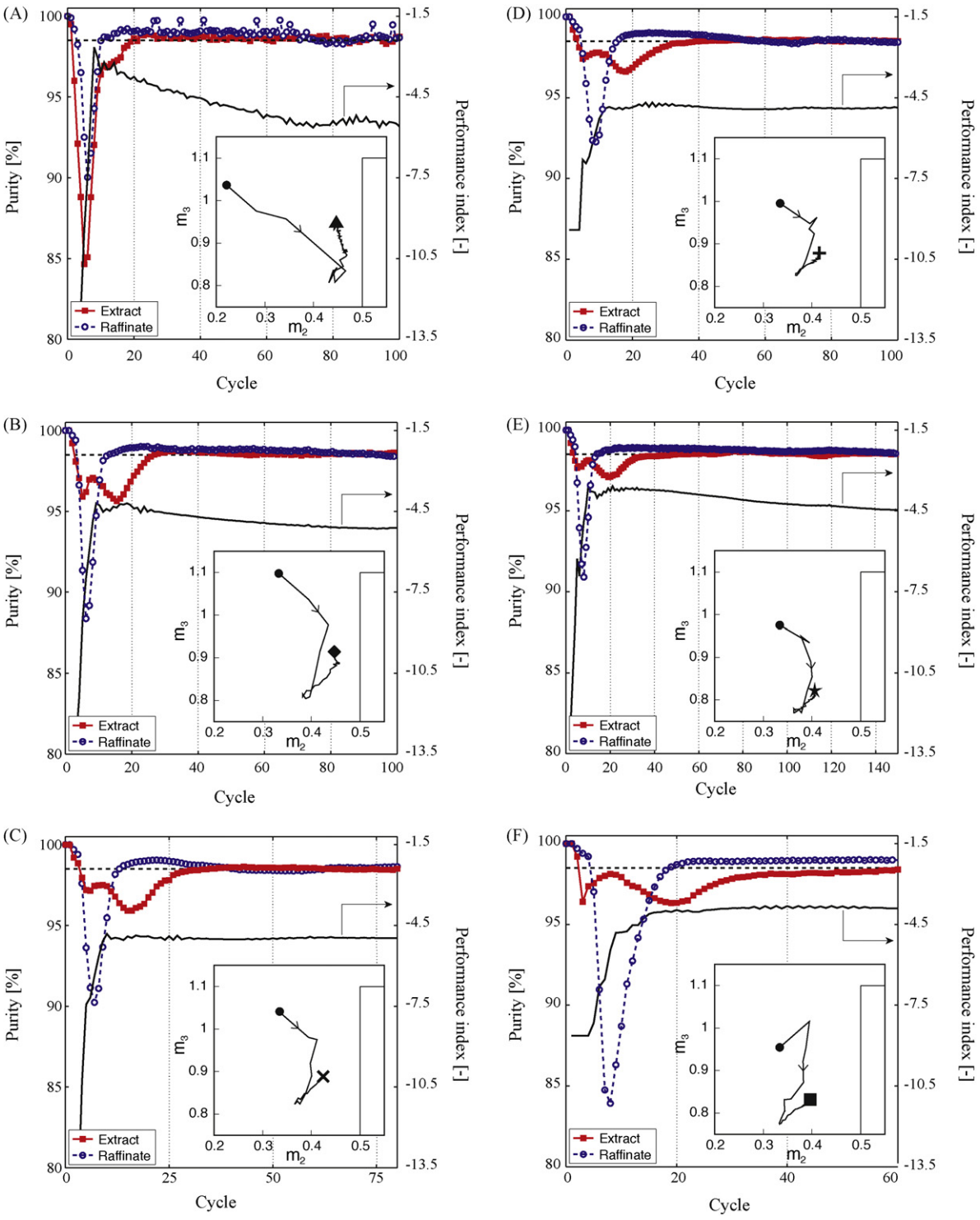

Fig. 4. Purities of the product streams and performance index (*P.I.*) as a function of time measured in cycles together with the trajectories in the (m_2, m_3) plane for runs A–F.

4.3. Case study 3: disturbance rejection

This experiment addresses one of the common disturbances occurring in an SMB plant, the malfunctioning of a pump. A rather challenging scenario of this type is selected for the current case study, namely the malfunctioning of the recycle pump, which is located before section 1 and therefore has an effect on the flow rates of all four sections of the SMB. The disturbance is simulated by changing on purpose the calibration of the recycle pump during the ongoing experiment. As a result the flow rates dictated by the controller for the next process cycle differ from those actually present in the unit. Hence, the controller is confronted with an SMB unit governed by different dynamics than before. Note that this change is unknown to the controller, and that the controller only notices the disturbance by its effect on the concentration measurements.

The steady state operation of run C ($c_T^F = 8$ g/L) was disturbed at cycle 80 by changing the calibration of the recycle pump, i.e. the recycle pump delivered 4% more flow than dictated by the controller. As a result, the flow rates in all four sections of the SMB were increased and the operating point in the (m_2, m_3) plane was

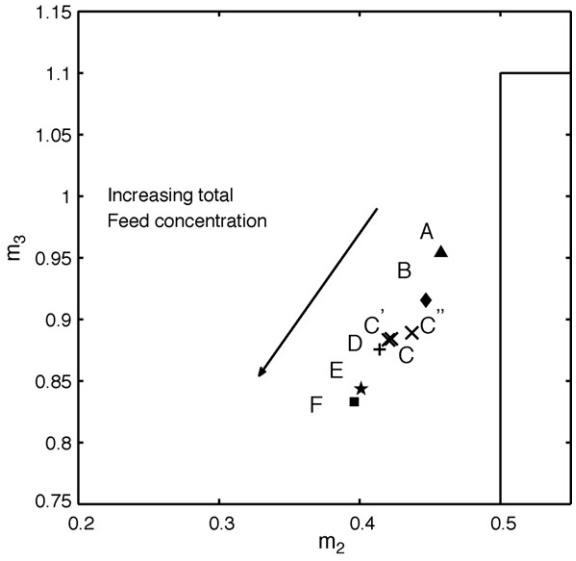

Fig. 5. Final operating points in the (m_2, m_3) plane for the runs A–F. The points C and C′ correspond to the results of case study 1 and 2, respectively.

shifted up to the right towards the region of pure extract, as shown in Fig. 7b. The corresponding *m*-values right after the disturbance and once the disturbance has been rejected are reported in Table 2 as run C″. Fig. 7a illustrates the time evolution of the extract and raffinate purities and the performance index *P.I.* as a function of the cycle number. Fig. 7c shows the sectional flow rates of the SMB unit as a function of the process time. In Fig. 7a it is observed that after the disturbance the raffinate purity drops to 83% and the extract purity increases to 100%, however within less than 20 cycles the controller recovers the purity specifications. The two main tasks of the controller are reflected in its disturbance rejection behavior. In order to recover the raffinate purity as fast as possible the controller reduces the flow rate in section 3 (see Fig. 7c); as a consequence the performance index *P.I.* increases, i.e. it gets worse. As soon as the purity specification is fulfilled the controller increases the flow rate in section 3 again, and as a result the *P.I.* gradually decreases, i.e. it improves. At the end of this process the flow rates Q_2, Q_3 and Q_4 as well as the feed flow rate are essentially the same as before the disturbance, as it can be seen in Fig. 7c or by comparing the final *m*-values reported in Table 2 for runs C and C″. On the other hand, the flow rate Q_1 reaches a value that deviates 4% from the

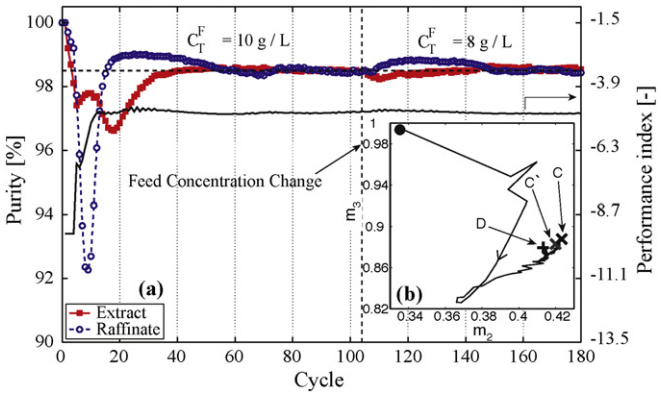

Fig. 6. Change of feed concentration during operation. (a) Purities of the product streams and performance index (*P.I.*) as a function of time measured in cycles. After 105 cycles the feed concentration is reduced from 10 g/L to 8 g/L. (b) Trajectory of the operating points for experimental run D. Final operating points C and C′ for the experiments in case study 1 and 2, respectively.

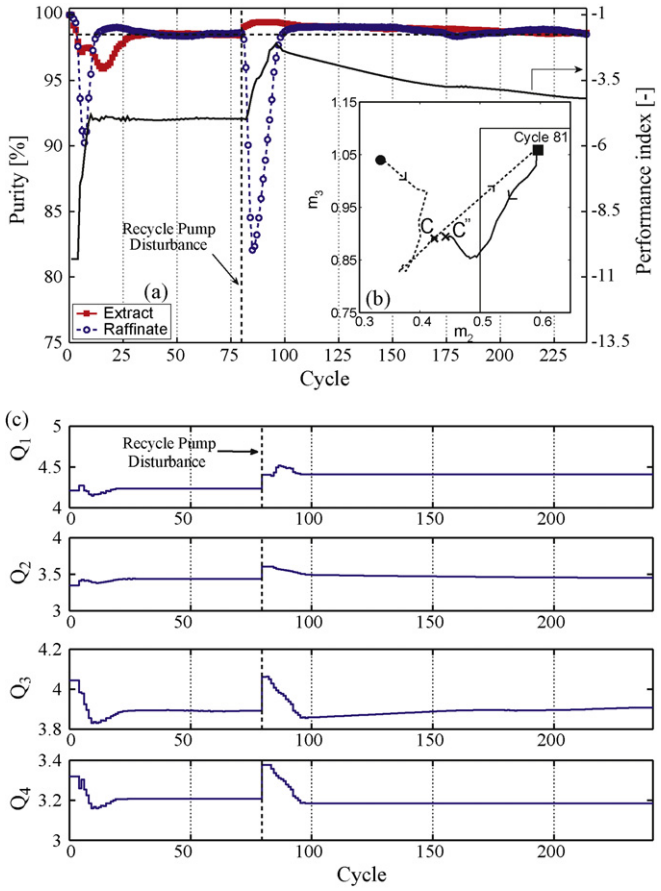

Fig. 7. Recycle pump disturbance. (a) Purities of the product streams and performance index (*P.I.*) as a function of time measured in cycles. After 80 cycles the recycle pump delivers 4% more than its set point. Total feed concentration $c_T^F = 8.0$ g/L. (b) Trajectory of the operating conditions: before disturbance (dashed line); after disturbance (solid line). (c) Internal flow rates of the SMB in ml/min for the rejection of the recycle pump disturbance.

previous one, see Fig. 7c again. This observation is consistent with the outcome of four control experiments reported previously [18], where an SMB separation problem with different initial operating flow rates reached different final values of Q_1 and Q_4 but the final values of Q_2 and Q_3 were the same in all four cases. This is also consistent with the simulation study comparing online optimizing control and offline optimization, where again the same values of Q_2 and Q_3 were attained by both optimization schemes, but differences up to 15% in the final Q_1 and Q_4 values were observed [15]. We attribute the reason of this behavior to the following facts. The benefit to reduce desorbent consumption by changing Q_1 has to compete with the penalty associated to the change of the same flow rate which is incorporated in the cost function of Eq. (12). When the current controller fulfills the purity specifications, the penalty on the control changes prevails over the former benefit and the *P.I.* after the disturbance turns out to be different than the one before.

4.4. Case study 4: purity requirements above 99%

The on-line monitoring system used in this work is based on HPLC measurements. This analytical technique allows for precise and accurate determination of the impurities. The following case study presents a scenario that exploits this advantage of the automated on-line HPLC monitoring system and specifies rather high minimal purities for the two product streams, namely 99.25%. A feed mixture of $c_T^F = 4$ g/L was fed to the SMB unit with initially

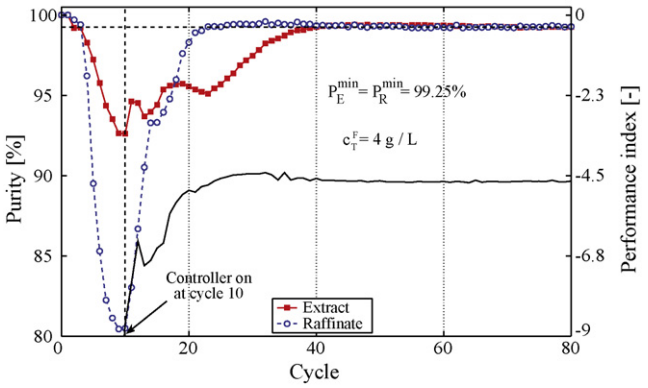

Fig. 8. Purities of the product streams and performance index (*P.I.*) as a function of time measured in cycles. Total feed concentration 4.0 g/L and purity specification 99.25%.

clean columns. The evolution of the purities and of the performance index is shown in Fig. 8. The controller was turned on at cycle 10 and within 30 cycles the purities are brought to the specified level and are held constant for the rest of the operation.

From Fig. 8 it is apparent that the controller manages to fulfill the purity specifications and the final value of the performance index is $P.I. = -4.65$. This value is higher than the final value of the performance index of experimental run B with a purity specification of 98.5% (see Fig. 4), i.e. $P.I. = -5.13$. This was to be expected since the feed flow rate has to be reduced to achieve higher purities, which in turn results in a worse value of the performance index.

5. Conclusions

In this paper, the experimental implementation of a 'cycle to cycle' optimizing controller in an SMB unit for chiral separations under nonlinear chromatographic conditions has been presented. The experiments were carried out in a 8-column laboratory scale SMB unit for the separation of a racemic mixture of guaifenesin enantiomers on Chiralcel OD stationary phase using ethanol as mobile phase.

A new automated on-line HPLC monitoring system was effectively used to measure the average concentration of the product streams, which are required as feedback information by the controller. This monitoring system overcomes the limitations imposed by optical detectors used in previous works to monitor the concentrations of chiral species. Its accuracy and reliability have been previously reported [18] and are evident from the quality of the purity measurements presented along this paper and from the 900 cycles of experiments reported in the case studies, which corresponds to 10 days of non-stop operation.

The experimental runs were designed to challenge the performance of the controller under nonlinear chromatographic conditions. The experimental results have clearly validated the most valuable asset of the 'cycle to cycle' controller developed in the last years: the controller can deliver the specified purities and improve the productivity with the knowledge of the linear adsorption behavior only even if the separation at stake is governed by an unknown nonlinear adsorption isotherm and despite major disturbances in the SMB unit. This is an important achievement since the time consuming task of determining the complete adsorption isotherm of a new mixture to be separated becomes redundant. The controller and the approach presented in this work offer a fast and reliable way to set up chiral SMB separations in a shorter time.

Nomenclature

c_i	concentration of species i [g/L]
H_i	Henry constants of species i
m_j	flow rate ratio in section j
n_{col}	number of columns
P	purity
PR	productivity [g/(min L)]
Q_j	volumetric fluid flow rate in section j [ml/min]
SC	solvent consumption [L/g]
t^*	switch time [min]
t_0	retention time of non-retained species [min]
$t_{R,i}$	retention time of component i [min]
V	column volume [ml]
V_j^D	dead volume in section j [ml]

Greek letters

ϵ^*	overall void fraction
λ_D, λ_F,	weighting factor in cost function

Subscripts and superscripts

A	more retained component
B	less retained component
ave	average
D	desorbent
E	extract
F	feed
i	component index
j	section index ($j = 1, \ldots, 4$)
max	maximum
min	minimum
R	raffinate

References

[1] M. Juza, M. Mazzotti, M. Morbidelli, Trends Biotechnol. 18 (2000) 108.
[3] E. Kloppenburg, E.D. Gilles, J. Process Control 9 (1999) 41.
[4] K.U. Klatt, F. Hanisch, G. Dunnebier, S. Engell, Comput. Chem. Eng. 24 (2000) 1119.
[5] K.U. Klatt, F. Hanisch, G. Dunnebier, J. Process Control 12 (2002) 203.
[6] H. Schramm, S. Gruner, A. Kienle, J. Chromatogr. A 1006 (2003) 3.
[7] C. Wang, K.U. Klatt, G. Dunnebier, S. Engell, F. Hanisch, Control Eng. Pract. 11 (2003) 949.
[8] A. Toumi, S. Engell, Chem. Eng. Sci. 59 (2004) 3777.
[9] I.H. Song, M. Amanullah, G. Erdem, M. Mazzotti, H.K. Rhee, J. Chromatogr. A 1113 (2006) 60.
[10] I.H. Song, S.B. Lee, H.K. Rhee, M. Mazzotti, Chem. Eng. Sci. 61 (2006) 1973.
[11] I.H. Song, S.B. Lee, H.K. Rhee, M. Mazzotti, Chem. Eng. Sci. 61 (2006) 6165.
[12] S. Engell, J. Process Control 17 (2007) 203.
[14] G. Erdem, S. Abel, M. Morari, M. Mazzotti, M. Morbidelli, Ind. Eng. Chem. Res. 43 (2004) 3895.
[15] C. Grossmann, M. Amanullah, M. Morari, M. Mazzotti, M. Morbidelli, Adsorption 14 (2008) 423.
[16] G. Erdem, M. Morari, M. Amanullah, M. Mazzotti, M. Morbidelli, AIChE J. 52 (2006) 1481.
[17] M. Amanullah, C. Grossmann, M. Mazzotti, M. Morari, M. Morbidelli, J. Chromatogr. A 1165 (2007) 100.
[18] C. Langel, C. Grossmann, M. Morari, M. Mazzotti, M. Morbidelli, J. Chromatogr. A 1216 (2009) 8806.
[19] M. Mazzotti, J. Chromatogr. A 1126 (2006) 311.
[20] G. Storti, M. Mazzotti, M. Morbidelli, S. Carrà, AIChE J. 39 (1997) 471.
[21] M. Mazzotti, G. Storti, M. Morbidelli, J. Chromatogr. A 769 (1997) 3.
[22] M. Mazzotti, Ind. Eng. Chem. Res. 45 (2006) 6311.
[23] C. Grossmann, M. Amanullah, M. Morari, M. Mazzotti, M. Morbidelli, AIChE J. 54 (2008) 194.
[24] C. Migliorini, M. Mazzotti, M. Morbidelli, AIChE J. 45 (1999) 1411.
[25] S. Katsuo, C. Langel, P. Schanen, M. Mazzotti, J. Chromatogr. A 1216 (2009) 1084.
[26] J.H. Lee, S. Natarajan, K.S. Lee, J. Process Control 11 (2001) 195.
[27] C. Grossmann, M. Amanullah, M. Mazzotti, M. Morbidelli, M. Morari, IFAC Symposium on Dynamics and Control of Process Systems, 2007.